ОБЪЕДИНЕННЫЙ
ИНСТИТУТ
ЯДЕРНЫХ
ИССЛЕДОВАНИЙ
Дубна

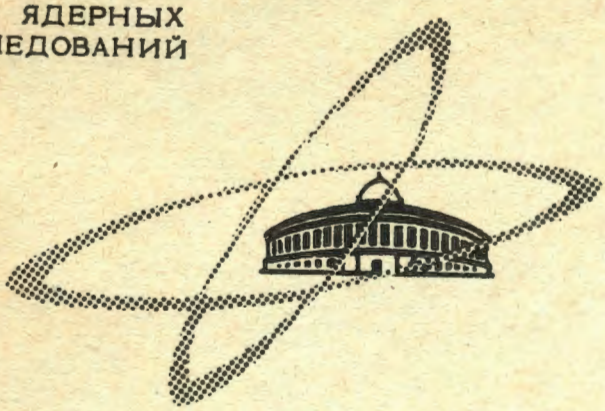

E14 - 3825

I.Natkaniec, K.Parliński, J.A.Janik,
A.Bajorek, M.Sudnik-Hrynkiewicz

LOCAL VIBRATIONS OF IMPURITY ATOMS IN COPPER AND LEAD

ЛАБОРАТОРИЯ НЕЙТРОННОЙ ФИЗИКИ

1968

E14 - 3825

I.Natkaniec, K.Parliński, J.A.Janik,*)
A.Bajorek, M.Sudnik-Hrynkiewicz

LOCAL VIBRATIONS OF IMPURITY ATOMS IN COPPER AND LEAD

*) Institute of Nuclear Physics, Kraków, Poland.

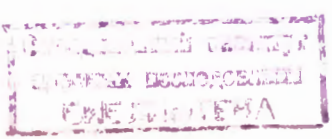

Натканец И., Парлиньски К., Яник Е.А., Байорек А.,
Судник-Хрынкевич М., E14-3825

Локальные колебания примесных атомов в меди и свинце

Методом неупругого рассеяния нейтронов были определены энергии локальных колебаний легких примесей атомов в следующих сплавах: Cu – Be /(42±2) мэв/, Cu – Mg /(34,5±2) мэв/, Pb – Na /(17±1) мэв/ и Pb–Mg/(16±1) мэв/. Структура исследуемых образцов была одновременно проверена методом упругого брэгговского рассеяния нейтронов. Для всех сплавов экспериментально полученные энергии локальных колебаний меньше значений, вычисленных в предположении, что силовые постоянные примесного атома равны силовым постоянным атомов матрицы. На основании экспериментальных значений энергий локальных колебаний дана оценка изменения силовых постоянных примесных атомов.

**Препринт Объединенного института ядерных исследований.
Дубна, 1967.**

Natkaniec I., Parliński K., Janik J.A., Bajorek A., E14-3825
Sudnik-Hrynkiewicz M.

Local Vibrations of Impurity Atoms in Copper and Lead

The inelastic neutron scattering technique was applied in determinations of the energy of the local vibrations of light impurity atoms in the alloys: Cu-Be/(42 ± 2) meV/, Cu-Mg /(34.5 ± 2) meV/, Pb-Na/(17± 1) meV/, and Pb-Mg/(16 ± 1) meV/. The structure of the examined samples was checked simultaneously by means of the elastic Bragg neutron scattering technique. For all alloys the energies of the local vibrations are lower than the values calculated with the assumption that the force constants of the impurity atom are equal to those of the host crystal. On the basis of the experimental values of the local vibration energy the change in the force constans for the impurity atoms was estimated.

**Preprint. Joint Institute for Nuclear Research.
Dubna, 1967.**

I. Introduction

The insertion into a crystal lattice site of an impurity atom of mass smaller than of the matrix atom may give rise to local vibrations of a frequency higher than the maximum of the vibrations of the crystal /1,2/. Experimental determination of the parameters of the local vibrations of light impurity atoms in the crystal lattice makes it possible to estimate directly the values of the impurity atom force constants and in alloys to estimate indirectly the variation in the conduction electron density. The results of the studies /3-6/ show that the method of inelastic neutron scattering may be particularly useful here. The purpose of this work, being a continuation of /7/, is to determine the energy of the local vibrations in binary alloys of copper and lead with light metals. Further aim of the work was to find samples for which the scattered neutron intensity would be high enough to allow subsequent determination of such parameters as the width, shift, and shape of the local vibration peak, which describe the anharmonicity introduced by the impurity atom.

II. Theoretical Remarks

The interaction potential of the atoms in a pure metal (and thus its force contstants) consists of the Coulomb potential of the bare ionic cores and the potential of interaction via the conduction electrons in which the interaction of electrons with an ionic core is described by a pseudopotential and the screening interaction is described by the dielectric constant of the metal. By means of a potential defined thus it is possible to calculate the dispersion curves of pure metals with satisfactory accuracy /8,9/.

The presence of the impurity atom introduces another local pseudopotential, characteristic of a given atom, and when the valencies differ it also gives rise to a change in the density of the conduction electrons around the impurity atoms (Friedel oscillations)/10/.

The frequencies of the local vibrations are given by the solutions to the equation,

$$| \bar{G}(\omega^2) \cdot \bar{\delta L} - \bar{1} | = 0 , \qquad (1)$$

where: $\bar{G}(\omega^2)$ is the Green function of the pure crystal /1/, and $\bar{\delta L}$ is the matrix defining the perturbation caused by the presence of the impurity atom. Its elements depend on differences between the force constants of the impurity atoms and the host atoms. If we assume that the force constants of the impurity atom are identical to those of the host atoms, then the frequency of the local vibrations, ω_ℓ , for a cubic crystal is given by the solution to the equation

$$\epsilon \omega^2 \int_0^{\omega_{max}} \frac{g(\omega_0)\, d\omega_0}{\omega^2 - \omega_0^2} = 1 , \qquad (2)$$

where: $\epsilon = 1 - \frac{m'}{m_0}$, m' is the mass of the impurity atom, m_0 is the mass of the host atom, and $g(\omega_0)$ is the frequency spectrum of the host lattice, ω_{max} is the maximum frequency of the host crystal vibrations.

The local vibrations can be observed by means of inelastic neutron scattering. The cross-section for the interaction between the neutron and the impurity atom and the lattice distortion caused by it is entirely incoherent. With an assumed lack of change in the force constants it is expressed for polycrystal of cubic symmetry by the formula /4/,

$$\frac{d^2\sigma}{d\Omega\, dE} = c\frac{k}{k_0} e^{-W} \frac{\kappa^2}{2m_0} \frac{1}{\omega_\ell} \left(D \frac{d\ell n\, \omega_\ell^2}{d\epsilon} + C\right) n_\ell \delta(\Delta E - \omega_\ell), \quad (3)$$

where:

$$D = [(1-\epsilon)\bar{A} - A_0]^2 + C_0 - (1-\epsilon)C, \quad (4)$$

$$\frac{d\ell n\, \omega_\ell^2}{d\epsilon} = \left\{\epsilon^2 \omega_\ell^4 \int_0^{\omega_{max}} \frac{g(\omega_0)\, d\omega_0}{(\omega_\ell^2 - \omega_0^2)^2} - \epsilon\right\}^{-1}, \quad n_\ell = \frac{1}{1 - e^{\omega_\ell / kT}}, \quad (5)$$

c is the impurity concentration, k, k_0, E and E_0 are the wave-numbers and energies of the scattered and incident neutrons, respectively, $\vec{\kappa} = \vec{k}_0 - \vec{k}$, $\Delta E = E_0 - E$, $\bar{A}$ and A_0 are the coherent neutron scattering lengths for the atoms of the host lattice and the impurity, and $4\pi C$ and $4\pi C_0$ are the incoherent cross-section of the atoms of the host lattice and the impurity.

The neutron scattering cross-section increases with increasing frequency of the local vibrations, for the function (5) grows rapidly when ϵ tends to unity. When there is a change in the force constants of the impurity atom respect to the host atoms, the value of the cross-section also changes. Notwithstanding, Eq. (3) is in general sufficient for estimating the intensity of the local vibration peak. Table I gives a comparison of the cross-section for neutron scattering on atoms of the host lattice and the impurity atoms.

III. Experimental Technique and Sample Preparation

The measurements were performed on the time-of-flight spectrometer operating in inverted-filter geometry at the IBR pulsed reactor (Fig.1). Details of the spectrometer for inelastic incoherent neutron scattering (arm I) have been presented in papers /11,12/. In accordance with the concept in papers /13/, arm II of the spectrometer was used for simultaneous measurement of the neutron diffraction patterns in order to check the sample structure.

The duration of the thermal neutron pulse was approx. 200μsec and the moderator-to-sample distance, L_1, was 20.4 m. Other spectrometer parameters during the measurements were:

I. Inelastic neutron scattering (arm I)
energy analyser: Be filter,
sample-to-detector distance: L_2 I = 0.94 m,
mean scattered energy 4.08 meV
resolution: $\frac{\Delta\lambda}{\lambda}$ = 8% for an energy transfer of 10 to 130 meV
scattering angle : $\Phi_1 = 90^\circ$.

II. Elastic neutron scattering (arm II)
Sample-to-detector distance: L_2 II = 0.95 m,
resolution $\frac{\Delta\lambda}{\lambda}$ = 1.5 to 2% for λ = 5 to 1 Å,
scattering angle: $\Phi_2 = 90^\circ$.

The distribution of inelastic neutron scattering for all the samples presented here display a strong peak at a neutron energy transfer of approximately 60 meV. A similar peak is also observed in the distribution of neutrons scattered inelastically on beryllium with large momentum transfer. In our case this kind of scattering takes place in the beryllium filter, in which only vertical layers of absorbing meterial spaced every 40 mm were inserted in order to have higher transmission. Neutrons which are removed from the beam due to Bragg scattering in the Be filter may become scattered inelastically on the beryllium and be recorded by the detector before

reaching the absorbing layer. Similar effects in the sample, namely, elastic Bragg scattering in the plane of the sample and subsequent inelastic multiphonon scattering of these neutron in the direction of the detector, give rise to a certain structure of the phonon peak of beryllium. The position of these weaker peaks in the scale of the scattered energy depends on the angle θ of sample alignment with respect to the incident beam direction.

These effects are negligibly small in the case of thin samples (from 0.1 to 1 mm) of substances containing hydrogen which scatter neutrons inelastically. This is the primary topic of work done with this spectrometer. For metal samples, primarily yielding elastic scattering, whose thickness is larger by an order of magnitude at the same transmission, the effects of multiple scattering (of the elastic--inelastic type) both in the sample and the Be filter become quite important. The effect due to the filter can be reduced considerably by the use of a gird of absorbing material, the spacings of which would be shorter than the mean free path for a neutron scattered inelastically in beryllium ($\approx$ 1.35 cm); however, this would greatly decrease the transmission of the filter because of the double collimation. Another way of abating this effect is to shift the incident neutron spectrum towards the lower energies. The sample effect can be eliminated by the use of an absorbing gird in the sample (which would also lower the intensity considerably) or, as mentioned, by making an appropriate choice of the angle θ .

The metals Li, Be, Na, and Mg, introduced as admixtures into copper or lead, form with them solid substitutional solutions of limited solubility /14/. Some of the data characterizing this solubility are given in Table I. It decreases rapidly with lower temperatures and at room temperature for the examined alloys did not exceed one per cent. Owing to the low value of the cross-section for neutron scattering with excitation of local vibtrations of the impurity atoms (see Table I), samples of impurity concentrations higher than one atomic per cent had to be used. The samples were prepared by melting the two metals in argon atmosphere in a weight ration appropriate

for the given concentration. The copper-based alloys were annealed in vacuum at approximately 700° C (Cu-Mg) and 800° C (Cu-Be) in order to homogenize the composition in the solid state, and then hardened. In order to obtain samples of the required dimensions ($\Phi \approx 20$ cm) shavings were made which were then pressed in a special mould and placed in aluminium containers. The lead-based alloys, after homogenization in the liquid phase, were poured into a mould, rapidly solidified and hardened. Following this, the samples were worked down to an identical thickness of approx. 6 mm by cutting off the upper and lower sides of the ingot. The lead alloys of concentrations near maximum solubilities were measured some three hours after preparation. The pure metal samples of copper and lead were made under the same conditions as the alloy samples. During the measurements the samples were placed in a cryostat and cooled down to the temperature of liquid nitrogen, i.e. 77°K. The transmission of the samples was about 85 per cent.

IV. Results of Measurements

Copper alloys

We had investigated the dynamics of $Cu_{0.98} - Be_{0.02}$ and $Cu_{0.98} - Be_{0.05}$ alloys about a year and a half previously /7/, soon after the samples had been prepared. A check of the sample structure made then did not reveal the presence of the other phase in these samples. In the distribution of the neutrons scattered inelastically on these alloys we observed an additional peak at an energy of approx. 42 meV, which was interpreted as corresponding to the excitation of local vibrations of Be atoms in the Cu lattice. Since in the early stages of the ageing process of supersaturated Cu-Be solid solutions was observed precipitation of linear and two-dimensional

distortions in the uniform structure of the solid solution (f.c.c. as for Cu) called the α phase, in the present measurements we attempted to determine whether perhaps the observed peak is due to the ageing effects of the alloys.

The ageing process of supersaturated Cu-Be solid solutions was studied in the papers /15/ by the anomalous X-ray scattering technique. It was shown that at room temperature it proceeds very slowly (some 5.5. years are needed for phase equilibrium to be achieved) and that at ageing temperature of up to about 170°C there is characteristic precipitation of linear and, subsequently, two-dimensional regions of thickness of approx. 25 Å and structure of the β' phase (ordered alloy of Cs Cl structure , a ≈ 2.70 Å). At higher ageing temperatures the anomalous effects of linear and two-dimensional diffraction vanish and at temperatures around 400°C equilibrium between the α and β' phases is reached within some hours. Samples annealed at temperatures higher than 800°C for several hours and then hardened did not reveal any traces of anomalous scattering.

In our experiment the $Cu_{0.98} - Be_{0.02}$ sample aged naturally at room temperature for about 1 ½ years and the $Cu_{0.95} - Be_{0.05}$ sample was annealed further before measurements in a vacuum furnace at 400°C, for about 48 hours. According to the papers /15/, we should expect in the $Cu_{0.98} - Be_{0.02}$ sample only linear and planar precipitates of β' phase structure , whereas in the $Cu_{0.95} - Be_{0.05}$ sample there should be separate blocks of β' phase crystallites in quantities corresponding to the state of α and β' phase equilibrium for the temperature of 400°C.

The diffraction patterns of the examined samples, a section of one of which is presented in Fig.2, confirms these expectations. The diffraction pattern of the $Cu_{0.98} - Be_{0.02}$ alloy sample (curve 3) is identical with that of the pure copper sample (curve 1) . The slight broadening of the peaks corresponding to the Bragg reflections from the α phase f.c.c. structure, as compared with the analogous peaks for pure copper, can be explained by the effect of anomalous scat-

tering on the precipitates distorting this structure , as described above. In the diffraction pattern of the $Cu_{0.98}-Be_{0.05}$ sample (curve 4) we see distinct peaks corresponding to the β' phase structure, while the peaks corresponding to the α phase structure are shifted somewhat; this enables us to estimate that the lattice parameter is contracted by 1 to 2 per cent relative to the lattice parameter of pure copper.

Figure 3 shows the distributions of neutrons scattered inelastically on the examined samples of copper alloys. The background is substracted and the measurement time and sample transmission are normalized, but the incident neutron beam intensity is not. In the curves 3 and 4, corresponding to the $Cu_{0.98}-Be_{0.02}$ and $Cu_{0.95}-Be_{0.05}$ alloys, respectively, we see an additional peak at a neutron energy transfer of approx. 42 meV which is not observed in the distribution of pure copper (curve 1). Comparison of the relative heights of this peak in the mesurements presented herein and those performed $1\frac{1}{2}$ years earlier /7/ show that it dropped by an estimated 15 per cent for the $Cu_{0.98}-Be_{0.02}$ sample any by approx. 30 per cent for the $Cu_{0.95}-Be_{0.05}$ sample. According to the formula (3), the Be atom concentration in the Cu lattice should decrease in the same ratio. This corresponds to the precipitation of approximately 0.2 per cent of the Be atoms from the α phase for the $Cu_{0.98}-Be_{0.02}$ sample and about 1.5 per cent for the $Cu_{0.95}-Be_{0.05}$ sample. The facts imply that the peak at 42 meV in the distributions of inelastic neutron scattering on Cu-Be alloys corresponds to the α phase structure hence, to local vibrations of the Be atoms in the crystal lattice of copper. The dynamics of the β' phase may be revealed by a slight broadening of the observed peaks, relative to the measurements made earlier. An explanation of this problem requires measurements with much better resolution and also measurements of the inelastic neutron scattering distribution for a sample of uniform β' phase structure.

Curves 2 in Figs. 2 and 3 correspond to the $Cu_{0.97}-Mg_{0.03}$ alloy. The diffraction pattern of this alloy reveals small traces of a Cu_2Mg

type structure. More substantial, however, is the fact that the peaks corresponding to the α phase structure (f.c.c. as for Cu) are shifted, indicating dilatation of the crystal lattice parameter by 1 to 2 per cent as compared with that of pure copper. As the radius of the magnesium atom is larger than that of copper (see Table 1), this is evidence that the Mg atoms occupy atom sites in the crystal lattice of copper.

In the distribution of the neutrons scattered inelastically on this sample we observe only an increase in the scattered intensity within the region of the maximum frequencies of the copper lattice vibrations. The shape of this distribution insinuates that in the sample there are vibrations of frequencies higher than the maximum frequency of atomic vibrations in copper. Dividing this distribution by that for copper, we get a curve whose maximum corresponds to a neutron energy transfer of approx. 34.5 meV. This value was assumed to be the energy of the local vibtations of Mg atoms in the copper lattice. An alloy of the composition $Cu_{0.99}-Mg_{0.01}$ was also examined. No difference between this sample and the copper sample was found within the accuracy of the measurements.

The copper sample, to which the curves 1 and Figs.2 and 3 correspond, was produced from 99.9 per cent pure electrolytic copper under conditions identical to those for the Cu-Mg alloys. The diffraction patterns for this sample and those Cu-Mg samples show insignificant traces of oxidation. The positions of the observed peaks corresponding to the CuO structure are indicated by arrows in Fig.2. The traces of oxidation in the Cu- Be alloys are smaller still.

Lead Alloys

Among the light metals which form solid solution with lead, sodium, whose atoms bear the closest resemblence to those of Pb as regards dimensions, has the highest solubility (see Table I). The Pb-Na solid solution (α phase) has face-centred cubic structure,

and the lattice parameter of lead (a= 4.9497 Å) is contracted with increased sodium concentrations /14/ even though the radius of Na atoms is greater than that of Pb atoms. When the sodium concentration exceeds maximum solubility, a β phase of the f.c.c. structure of the Cu_3Au type ordered alloy (a=4.88 Å) is precipitated. The range of homogeneity of this phase lies within 26.5. to 35 at % Na, hence, it does not include the Pb_3Na composition /16/.

We examined the Pb-Na alloys in the 1 to 10 at.% Na concentration range. The neutron diffraction data of samples of concentrations lower than 5 at.% Na, measured less than two months after sample preparation, did not reveal any traces of the β phase. The diffraction pattern of sample with approx. 10 at.% Na taken immediately after the sample had been prepared had traces of peaks corresponding to the β phase structure. These peaks appeared much more distinctly after this sample was aged for one month at a temperature of about 40°C. If we compare the intensities of the peaks corresponding to the α and β phases, we can estimate that the β phase content in the aged sample does not exceed 5 per cent (95 per cent of the α phase would correspond to a $Pb_{0.91}-Na_{0.09}$ composition). Differences between the inelastic neutron scattering distributions measured under identical conditions did not exceed the accuracy of the measurements. With an increase of the sodium concentration in the alloy we also observe a slight shift of the peaks corresponding to the α phase structure. For the $Pb_{0.90}-Na_{0.10}$ sample it corresponds to a contraction of the lattice parameter of approx. 1 per cent. These facts imply that the effects observed in the inelastic neutron scattering distribution correspond to the α phase structure in which the Na atoms occupy isolated sites in the crystal lattice of lead.

In Fig.4 we have a comparison of the distributions of neutrons scattered inelastically on lead and some Pb-Na samples of different concentrations. In the lead distribution (curve 1) we can distinguish peaks at neutron energy transfers of about 5 meV and about 8.5 meV, which stand in good agreement with the maxima in the fre-

quency spectra of lead [17,18]. The severe drop in the neutron intensity at the energy transfer of approx. 10 meV corresponds to the limit of the lead frequency spectrum. The reason why the peak at the energy of approx. 60 meV appears is expounded in Sec.III. In the distributions of the alloys we see an additional peak beyond the limit of the lead frequency spectrum, the amplitude of which is proportional to the concentration of Na atoms in the sample. This peak corresponds to a neutron energy transfer of about 17 meV and, in accordance with what has been said about the sample structure, it is interpreted as due to the excitation of local vibrations of the Na atoms in the crystal lattice of lead. The width of this peak, being approximately 9 per cent, is in conformity with the spectrometer resolution at this energy [11]. By comparing the distribution shown in Fig.4 in the range of the normal vibrations for lead we see that with increased concentration of Na atoms there is a rise in the scattered intensity at the limit of the frequency spectrum. This implies that in the region of the normal vibrations of lead there is an increased probability of excitation of high-frequency vibrations.

The solubility of magnesium in the solid phase of lead is much more limited than of sodium (despite similar rations of atomic radii), as the Mg atoms form with Pb an electronic bond, Mg_2Pb, of metallic properties. The structure of this compound is of the CaF_2 type (a= 6.85 Å).

We examined the Pb-Mg alloy in the concentration range from 1 to 5 at.% Mg. In the $Pb_{0.99} - Mg_{0.01}$ and $Pb_{0.97} - Mg_{0.03}$ samples, not hardened after moulding and measured some two months after preparation, there was no additional peak beyond the limit of the natural vibrations of lead. Only a slight rise in the intensity of the scattered neutrons was observed in the region of the maximum frequences of the lead vibrations. The diffraction patterns of these samples revealed the presence of an Mg_2Pb type structure. In the $Pb_{0.95} - Mg_{0.05}$ sample, hardened immediately after solidification and cooled to the temperature of liquid nitrogen some two hours after preparation, we observed an additional peak at a neutron energy

transfer of approx. 16 meV, which was assigned to the excitation of the local vibrations of the Mg atoms. A strong rise in the scattered intensity was observed in the high-frequency region of the normal vibrations of lead. The diffraction pattern of the sample showed traces of an Mg_2Pb structure in quantities not higher than for the $Pb_{0.97} - Mg_{0.03}$ sample.

The region of lithium solubility in solid lead is even more restricted owing to the considerable difference of the atomic radii and valencies. The diffraction patterns of the examined samples of $Pb_{0.99} - Li_{0.01}$ and $Pb_{0.97} - Li_{0.03}$ compositions, hardened after solidification, show the presence of a $PbLi$ phase of b.c.c. structure of the $CsCl$ type (a=5·25 Å). In the distributions of neutrons scattered inelastically on these samples only the effects of neutron absorption by Li atoms are observed. No effects of neutron scattering on Li atoms exceeding the accuracy of the measurements were found. To observe them the effect-to-background ratio would have to be improved by increasing the incident beam intensity and the effect due to Be filter must be eliminated.

V. Discussion

In all the examined alloys the experimentally determined energy of the local vibrations of light impurity atoms is lower than the value calculated with the assumption that the force constans around the impurity atom remain unchanged (Eq.(2)). Table II gives a comparison of the local vibration energies calculated for different frequency spectra of copper and lead. The greatest effect on the calculated values of the local vibration energy is borne by the high-frequency vibrations of the host crystal lattice. An illustration of this fact are the differences in the results calculated for the Sinha and Debye spectra, in which the Debye limit frequency for copper was taken

to be equal to that of the Sinha spectrum. The assumed limit frequency of the Debye spectrum for lead corresponds to 88°K. The most realistic frequency spectra are: the Sinha spectrum for copper /21/ and the Stedman spectrum for lead /18/, calculated from the experimentally determined dispersion curves for these metals.

In order to assess the change in the force constants from the experimentally determined energy for the local vibrations of the impurity atom, we shall make use of the approximation of an extremely light impurity. With this assumption the nondiagonal elements of the $\bar{G}(\omega^2)\delta\bar{L}$ matrix are negligible. The local frequency will be given in the form of the following integral equation (for cubic crystals),

$$[\epsilon\omega^2 - p\int_0^{\omega_{max}} \omega_0^2 g(\omega_0)\,d\omega_0]\int_0^{\omega_{max}} \frac{g(\omega_0)\,d\omega_0}{\omega^2 - \omega_0^2} = 1 \quad , \tag{6}$$

where:

$$p = 1 - \frac{\Phi(00)}{\Phi^0(00)} \quad , \quad \Phi^0(00) = m_0 \int_0^{\omega_{max}} \omega_0^2 g(\omega_0)\,d\omega_0 \quad .$$

$\Phi^0(00)$ and $\Phi(00)$ are the force constants of the host atoms and impurity atoms, respectively. The impurity atom is at the site $\ell = 0$. The parameter p defines the magnitude of the change in the force constants of the impurity atom in the zeroth coordination sphere. Its value for various frequency spectra are given in Table II.

This approximation can also be applied for rather heavier impurities, but the perturbation caused by the impurity should spread out to larger distances and at the same time the change of the force constants of the first coordination spheres should be negligible, i.e.

$$|\Delta\Phi(0\ell)| < |\Delta\Phi(00)| \quad , \text{ where } \ell > 0 \quad .$$

The force constants of the zeroth coordination sphere is associated with the remaining ones by the relationship

$$\Phi(00) = -\sum_{\ell} \Phi(0\ell) \quad . \tag{7}$$

A better approximation would be obtained with a model in which only the force constants of the zeroth and first coordination spheres become changed. Their change can be determined from the experimental value of the local vibration energy and the dispersion curves of the host crystal (22). For beryllium atoms in copper the result of such calculations is:

$$p = \frac{\Delta|\Phi(00)|}{|\Phi(00)|} \approx \frac{\Delta|\Phi(01)|}{|\Phi(01)|} \approx 70\% \quad .$$

The estimation of the contribution of the long-range forces of Coulomb, ion-electron, and electron-electron interactions (causing a change in the force constants in the higher-order coordination spheres) gives the following assessment of the changes in the force constants for this alloy (22),

$$\frac{\Delta|\Phi(00)|}{|\Phi(00)|} = 65\% \quad , \quad \frac{\Delta|\Phi(01)|}{|\Phi(01)|} = 55\% \quad .$$

A comparison of these results with the values of the parameter p for Cu-Be in Table II shows the differences in the estimate of p in dependence on the model assumed. Unfortunately, a complete solution of Eq.(1) which would give an exact value for the local frequency is impossible and a simplifying model must be used.

Determination of the energy of the vibrations of light atoms in ordered phases of the investigated alloys should enable us to assess the effect of the force constants change of the higher-order coordination spheres on the local vibration energy, and also facilitate the choice of a model corresponding closer to the actual situation in a crystal. No changes exceeding the measurement accuracy were observed in the local vibration energy as a function of impurity atom concentration within the range of the solid solution phase.

In order to get more precise and complete information on the dynamics and interaction of atoms in the crystals of metals measurements with much better resolution should be made. Of the alloys

discussed here, the Cu-Be and Pb-Na alloys are best suited for this type of research, owing to the high intensity of neutron scattering and the structure of the solid phase. The time-of-flight technique and the inverted - filter geometry is convenient for this type of research, as it permits simultaneous measurement of the structure and the dynamics of the sample.

In conclusion the authors express their gratitude to Professor H. Niewodniczanski and Professor F.L.Shapiro for their interest in this work, and to Professor B.Buras for discussion concerning the methods of checking the sample structure.

References

1. A.A.Maradudin, Solid State Physics, 18, 274 (1966); 19, 2(1967).
2. И.М.Лифшиц, УФН, 88, 617 (1964).
3. Ю.Каган, Я.Иосилевский, ЖЭТФ, 44, 1375 (1963).
4. М.А.Кривоглаз, ЖЭТФ, 40, 567 (1961).
5. R.J.Elliot, A.A.Maradudin, Inelastic Scattering of Neutrons, IAEA, Vienna, 1965, p.225.
6. K.Parliński, Postępy Fizyki, 16, 667 (1965).
7. I. Natkaniec, K.Parliński, A.Bajorek, M.Sudnik-Hrynkiewicz, Phys. Lett., 24A, 517 (1967).
8. Е.Г.Бровман, Ю.Каган, ЖЭТФ, 52, 557 (1967).
9. A.O.E.Animalu, F.Bonsignori, V.Bortolani, Nuovo Cimento, Vol. 64B, 159 (1966).
10. J.Friedel, Phys. Mag. Suppl., 3, 496 (1954); Nuovo Cimento , Suppl., 7, 287 (1958).
11. A.Bajorek , T.A.Machekhina, K.Parliński, F.L.Shapiro, Inelastic Scattering of Neutrons, IAEA, Vienna, 1965, p.519 .
12. K. Parliński, M.Sudnik-Hrynkiewicz, A. Bajorek, J.A.Janik, W.Olejarczyk, Research Applications of Nuclear Pulsed Systems, IAEA, Vienna, 1967, p.179.

13. B,Buras, Report No 702/ II/PS (1966), Institute of Nuclear Research, Świerk, Poland; Research Applications of Nuclear Pulsed Systems, IAEA, Vienna, 1967, p.17.
14. M.Hansen, K.Anderko, Constitution of Binary Alloys, McGraw - - Hill Book Company, New York, Toronto, London, 1958.
15. А.М.Елистратов, С.Д.Финкельштейн, А.И.Пашилов, ДАН СССР, 68, 1017 (1949); А.М.Елистратов, С.Д,Финкельштейн, Т.Ю.Гольдштейн, ДАН СССР, 88, 669 (1953); А.М.Елистратов, ДАН СССР, 101, 69 (1955).

16.Е.С.Макаров, З.В.Попова, Изв. АН СССР, ОХН, 337 (1951).
17. G.Gilat, Solid State Comm., 3, 101 (1965).
18. R.Stedman, L.Almquist, G.Nilson, Phys. Rev., 162, 549 (1967).
19. E.H. Jacobsen, Phys. Rev., 97, 654 (1955).
20. R.B.Leighton, Rev. Mod. Phys., 20, 165 (1948).
21. S.K.Sinha, Phys. Rev., 143, 422 (1966).
22. В.Б.Приезжев, Препринт ОИЯИ, 3746, Дубна, 1968.

Received by Publishing Department
on April 18, 1968.

Table I.

Alloy	$\frac{m'}{m_o}$	ε	$4\pi\Gamma^2$	$4\pi D$	$\frac{r_{host} - r_{imp.}}{r_{host}}$	Max. solubility c_{max} /at. %/	Temp. of max. solubility ^oC
Cu - Be	0·142	0·858	7·0	4·5	+ 0·133	16·4	866
Cu - Mg	0·383	0·617	7·0	1·3	- 0·250	7	722
Pb - Na	0·111	0·889	11·58	2·66	- 0·063	12	300
Pb - Mg	0·117	0·883	11·58	2·40	+ 0·086	6	253
Pb - Li	0·096	0·904	11·58	1·77	+ 0·131	3	235

Table II.

Alloy	Local vibration energy		$\frac{E_{th} - E_{exp}}{E_{th}}$	Change in force const. from Eq./6/	References regarding $g(\omega_o)$
	Experimental value	Calculated from Eq./2/			
Cu - Be	(42 ± 2) meV	54°0 meV	22%	0°43	E.H. Jacobsen /19/
		56°1 meV	25%	0°50	R.B. Leighton /20/
		57°9 meV	28%	0°56	S.K. Sinha /21/
		61°5 meV	31%	0°60	Debye spectrum
Cu - Mg	(34°5 ± 2) meV	34°2 meV	0%	0°00	E.H. Jacobsen
		35°9 meV	3%	0°10	R.B. Leighton
		37°5 meV	8%	0°22	S.K. Sinha
		38°7 meV	11%	0°27	Debye spectrum
Pb - Na	(17 ± 1) meV	18°75 meV	9%	0°16	Debye spectrum
		19°25 meV	12%	0°23	R. Stedman /18/
		19°70 meV	14%	0°27	G. Gilat /17/
Pb - Mg	(16 ± 1) meV	17°9 meV	11%	0°20	Debye spectrum
		18°7 meV	14%	0°30	R.Stedman
		19°2 meV	17%	0°34	G. Gilat

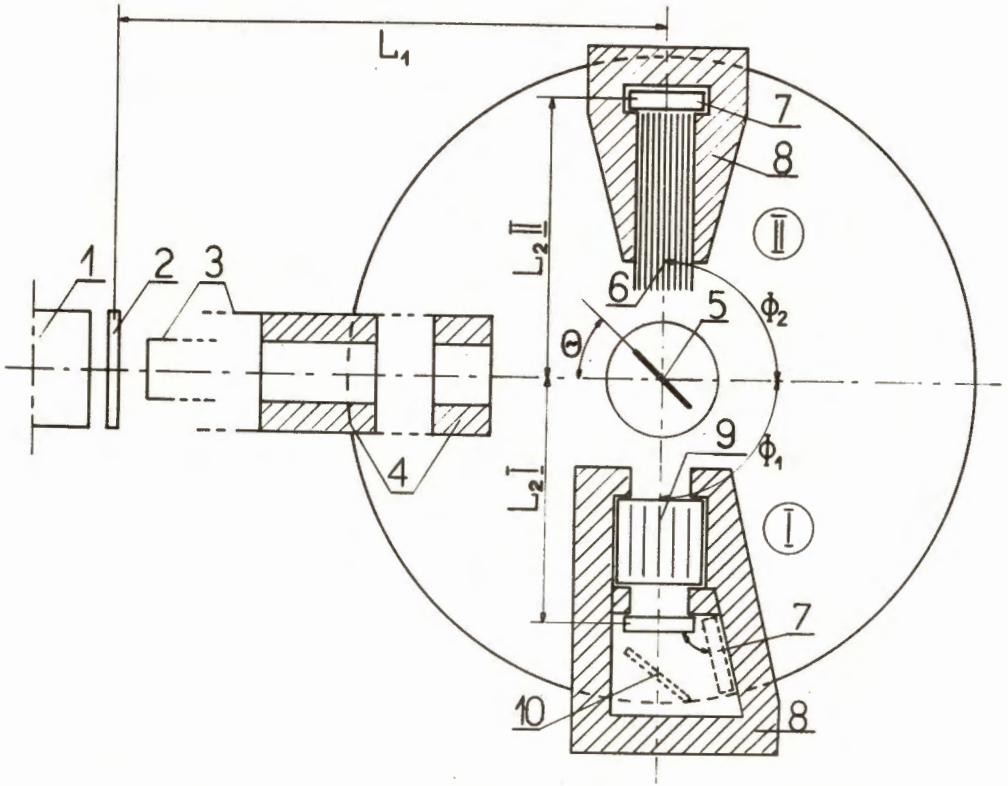

Fig.1. 1. reactor core, 2.moderator, 3. vacuum tubes, 4. collimators for incoming beam, 5. sample in low-temperature cryostat, 6. collimator for diffraction study, 7. detectors (trays of BF_3 counters), 8. shielding, 9. beryllium filter with collimating cadmium inserts, 10. zinc single crystal.

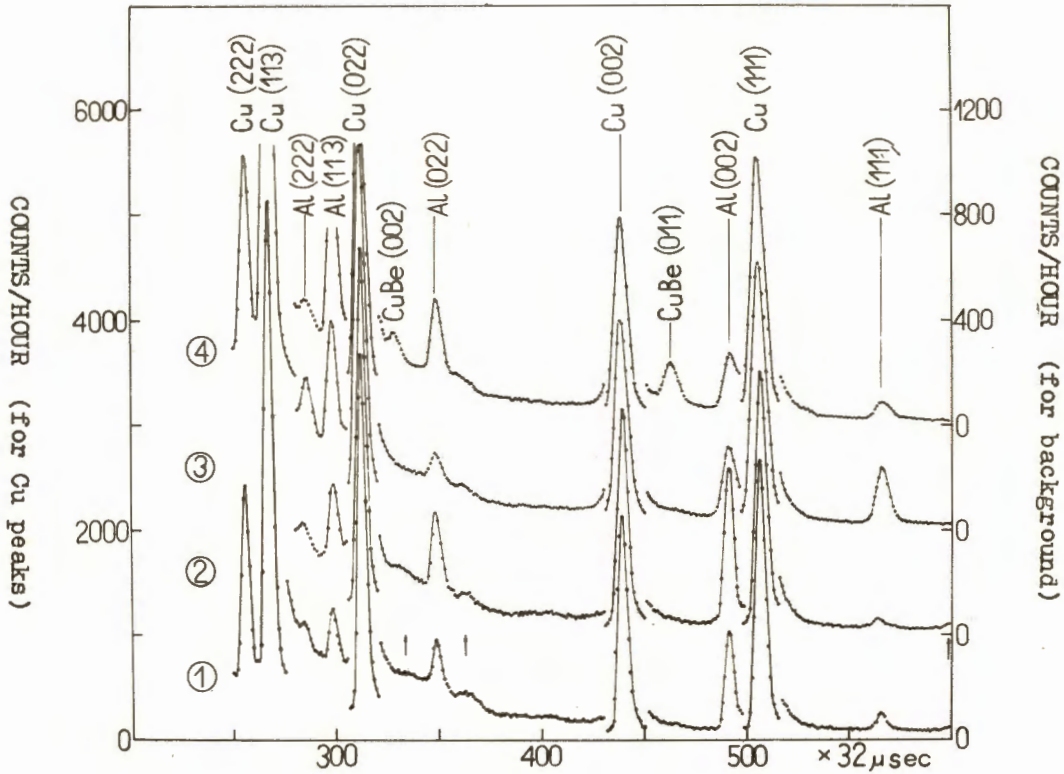

Fig.2. Section of the diffraction pattern for the investigated copper-based alloy samples: 1. Cu, 2. $Cu_{0.97} - Mg_{0.03}$, 3. $Cu_{0.98} - Be_{0.02}$ 4. $Cu_{0.95} - Be_{0.05}$.

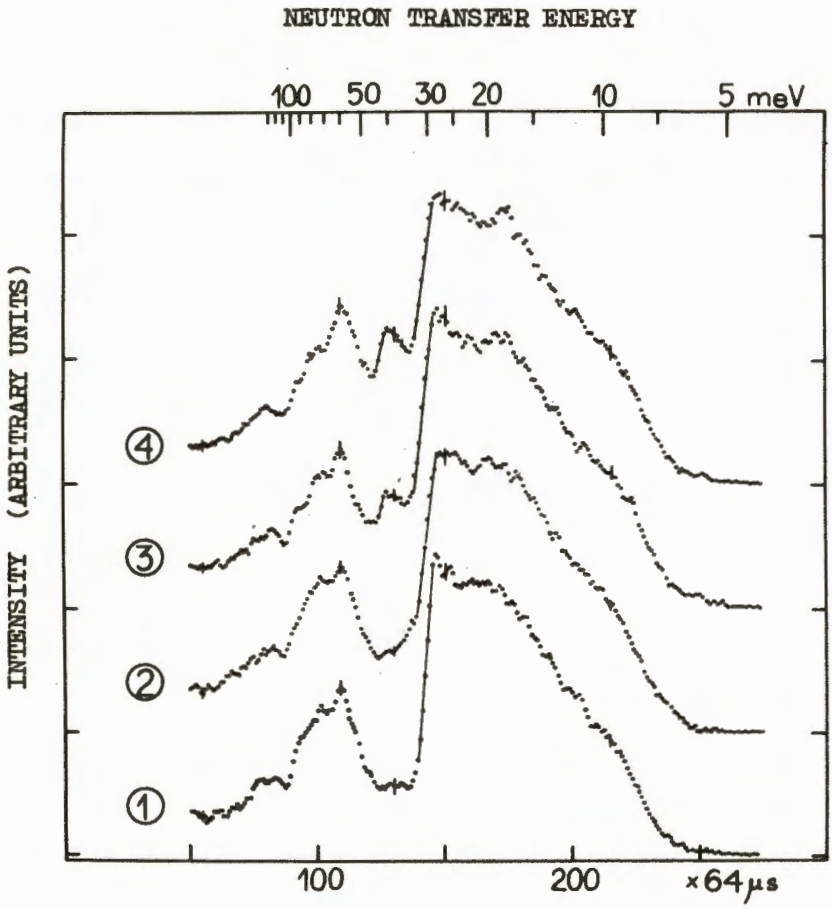

Fig. 3. Inelastic neutron scattering distributions for the investigated copper-based alloy samples: 1. Cu, 2. $Cu_{0.97}-Mg_{0.03}$, 3. $Cu_{0.98}-Be_{0.02}$, 4. $Cu_{0.95}-Be_{0.05}$

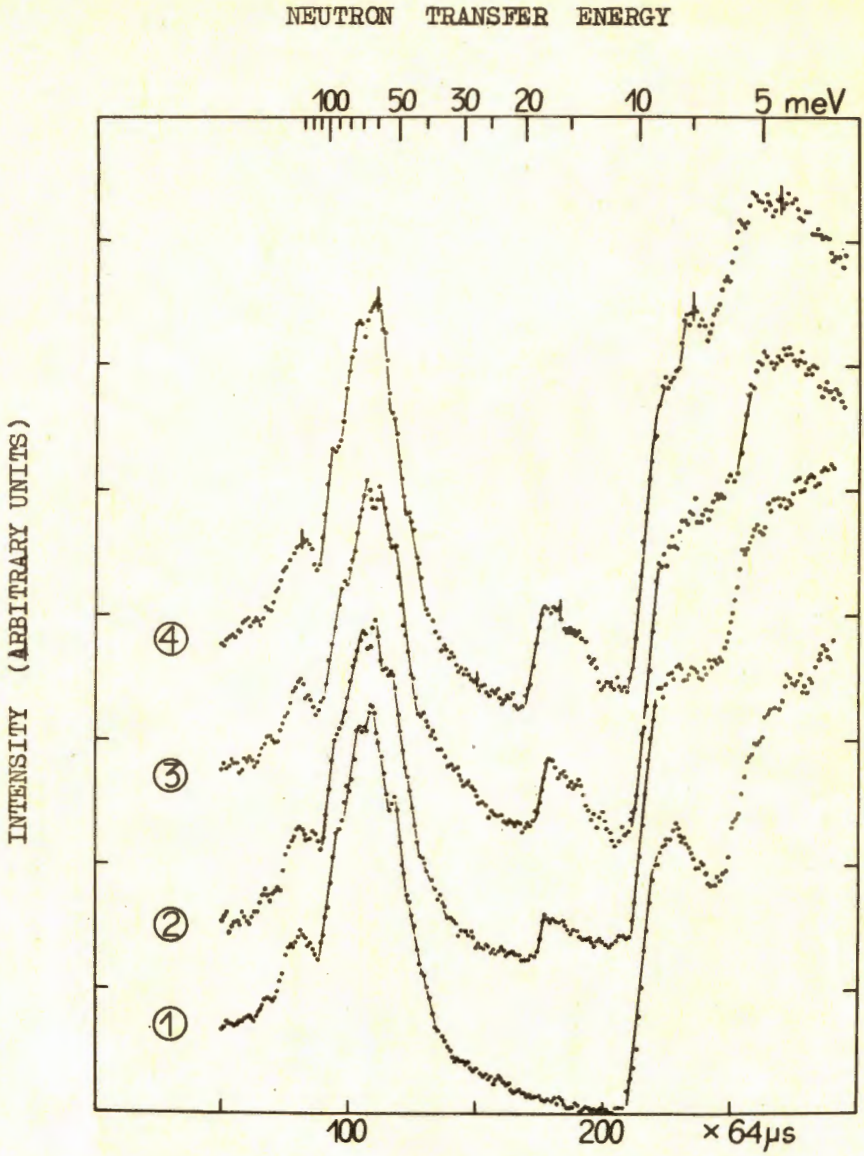

Fig.4. Inelastic neutron scattering distributions for the investigated lead-sodium alloy samples: 1. Pb, 2. $Pb_{0.98}-Na_{0.02}$, 3. $Pb_{0.95}-Na_{0.05}$, 4. $Pb_{0.90}-Na_{0.10}$